Compression-Molded Polyurethane Block Copolymers. 2. Evaluation of Microphase Compositions

Jeffrey T. Koberstein* and Louis M. Leung†

Department of Chemical Engineering and Institute of Materials Science, University of Connecticut, Storrs, Connecticut 06269-3136

Received October 3, 1991; Revised Manuscript Received July 6, 1992

ABSTRACT: Two general methods are presented for the determination of microphase compositions of pseudo-two-phase segmented block copolymers. The development is based upon combined differential scanning calorimetry (DSC) and small-angle X-ray scattering (SAXS) analyses. The first method employs an extension of the Couchman equations to relate microphase compositions to glass transition temperatures. The second procedure uses a modified Fox formalism for this purpose. Microphase compositions are estimated by these methods for a series of polyurethane segmented copolymers synthesized from 4,4′-diphenylmethane diisocyanate (MDI), 1,4-butanediol (BDO), and poly(oxypropylene glycol). The self-consistency of the calculations is checked by comparing measured and estimated electron density variances. The results of the extended Couchman analysis are found to be inconsistent with experimental data. The modified Fox treatment leads to results which are qualitatively self-consistent. Calculated microphase compositions are used to estimate the critical hard-segment sequence length below which hard sequences dissolve within the soft microphase. The estimated critical lengths fall in the range of 5–7 (MDI residues per sequence). The overall phase mixing behavior and morphology are shown to be in qualitative agreement with the predictions of the Koberstein–Stein model for hard microdomain structure.

I. Introduction

The versatile mechanical properties of segmented polyurethane elastomers are generally attributed to the formation of a microphase-separated structure that arises due to incompatibility of the glassy hard-segment and rubbery soft-segment sequences. In most investigations, the degree of microphase separation has been found to be incomplete. That is, microdomains are not pure as a result of intersegmental mixing. Mixing within the soft microphase is reflected by an elevation in its glass transition temperature as compared to the pure component value.[1,2] The dissolution of hard segments within the soft microphase is associated with the broad distribution of hard-segment sequence lengths inherent from the polymerization reaction.[3] Shorter hard segments have a lower driving force for microphase separation and might be expected to remain mixed within the soft microphase. Preferential solvation of shorter sequences provided the basis for the model for polyurethane morphology developed by Koberstein and Stein.[4] This model predicts that the hard microdomain thickness is controlled by the hard–soft-segment compatibility, being related to the shortest phase-separated hard-segment sequence. A recent small-angle X-ray scattering (SAXS) investigation[1] provided strong evidence in favor of this model by demonstrating a qualitative correlation between hard microdomain structure and the soft microphase glass transition temperature. The soft microphase composition and associated glass transition temperature is an important parameter to be controlled since it has a direct influence on the low-temperature extensibility and modulus of the material.

The composition and glass transition temperature of the hard microphase is equally important due to its influence on the heat distortion or deflection temperature and plateau modulus. Hard microdomain glass transition temperatures estimated from differential scanning calorimetry (DSC)[2,5] or thermomechanical analysis[2,6,7] are found to be lower than that of the pure hard segment,[8] suggesting the presence of "dissolved" soft-segment units. These dissolved units most probably result from non-equilibrium entrapment of soft-segment sequences of the multiblock chain.

The importance of microphase separation in controlling polyurethane properties provides strong motivation for the development of methods to characterize the degree of microphase separation. A number of such methods have consequently appeared. Camberlin and Pascault proposed a method based solely on the results of DSC measurements.[9] In their treatment, dissolved hard segments were assumed to have a negligible contribution to the change in heat capacity at the soft microphase glass transition. This assumption is inconsistent with use of the Fox equation,[10] since this equation is based upon the assumption that heat capacity contributions are equivalent for both constituents as has been emphasized by Couchman.[11] A similar DSC annealing–quenching method was employed to construct an apparent microphase composition–temperature diagram for a segmented polyurethane block copolymer.[5] Analysis of the experimental data also suggested that the heat capacity contribution from dissolved hard segments was negligible as assumed by Camberlin and Pascault but did not resolve the apparent discrepancy with theory. Methods for the determination of microphase compositions from the results of scattering experiments have also appeared.[1] In general, these methods require either an additional experiment, fitting a model, or making restrictive assumptions in order to arrive at a solution.

In this paper, we present methods for the determination of microphase compositions in two-phase systems that are based upon a combined analysis of DSC and SAXS experiments. The methods are applied to the experimental data for the series of polyurethane elastomers described in the preceding article but are generally applicable for all pseudo-two-phase materials.

II. Theory

DSC Analysis of Glass Transition Temperatures. Thermal analysis has been applied widely to study miscibility in polymer blends. The goal of these inves-

* To whom correspondence should be addressed.
† Present address: Department of Chemistry, Hong Kong Baptist College, 224 Waterloo Road, Kowloon, Hong Kong.

0024-9297/92/2225-6205$03.00/0

tigations is generally to relate glass transition temperatures (T_g) to the overall blend composition and characteristic thermal properties of the blend constituents. A number of equations that express this relationship have appeared,[10,11,15-17] both of empirical and thermodynamic origin. Equations of similar form have been developed to describe the glass transition behavior of copolymers.[18,19] The most general of these theories are those of Couchman.[11,17,18] The Couchman equations have been shown to reduce to the more familiar empirical relations, given appropriate assumptions. The basis of the Couchman theory for random copolymers is the consideration of individual contributions associated with the various diad species that comprise the chain. Each diad ij (e.g., monomers i and j) makes a contribution $T_{g_{ij}}$ to the glass transition temperature (T_g) and $\Delta C_{p_{ij}}$ to the change in heat capacity (ΔC_p) at T_g. In the original development, the equations predicting the overall T_g and ΔC_p for a copolymer containing m species i and j take the form

$$\ln T_g = \frac{\sum_i^m \sum_j^m w_{ij} \Delta C_{pij} \ln T_{g_{ij}}}{\sum_i^m \sum_j^m w_{ij} \Delta C_{p_{ij}}} \tag{1}$$

and

$$\Delta C_p = \frac{\sum_i^m \sum_j^m w_{ij} \Delta C_{p_{ij}}}{\sum_i^m \sum_j^m w_{ij}} \tag{2}$$

The w_{ij} terms refer to the weight fractions of ij diads. They may be determined from the chemical composition of the copolymer and the reactivity ratios.

In the particular case of segmented polyurethane elastomers, these equations can be applied to characterize the glass transition process of the soft microphase. The soft microphase consists of soft segments connected by covalent bonds to dissolved hard-segment units. This "mixed" soft microphase can thus be treated as a single-phase copolymer system comprised of three component species. These species are the soft segment (s), the diisocyanate residue (d), and the chain extender residue (c). If the soft-segment prepolymer is treated as a single species (ds), the polyurethane chain dissolved within the soft microphase presents the structure of an alternating copolymer represented by $-[(dc)_n ds]-$, where n is the average number of diisocyanate residues per dissolved hard segment. Furthermore, this copolymer chain contains no like diads and only unlike diads of the type soft segment/diisocyanate (type sd) or diisocyanate/chain extender (type dc). The Couchman equations for the polyurethane soft microphase may therefore be written as

$$\ln T_g = \frac{w_{sd} \Delta C_{p_{sd}} \ln T_{g_{sd}} + w_{dc} \Delta C_{p_{dc}} \ln T_{g_{dc}}}{w_{sd} \Delta C_{p_{sd}} + w_{dc} \Delta C_{p_{dc}}} \tag{3}$$

and

$$\frac{\Delta C_p}{W_1} = \frac{w_{sd} \Delta C_{p_{sd}} + w_{dc} \Delta C_{p_{dc}}}{w_{sd} + w_{dc}} \tag{4}$$

Here ΔC_p is the heat capacity change per gram of the total polymer at the soft microphase glass transition temperature and W_1 is the overall weight fraction of the soft (mixed) microphase. Further simplification of the equation may be accomplished by approximating terms of the type $\ln T_{g_{ij}}$ by $1/T_{g_{ij}}$, as has been suggested by Couchman.

If the dissolved copolymer may be considered random, that is, if the polymerization reaction proceeds statistically, definition of the diad fractions is straightforward. The weight fraction of each diad is simply related to the product of the probabilities of finding each species

$$w_{ij} = \frac{f_i f_j M_{ij}}{M} \tag{5}$$

where M is the average molecular weight of the dissolved chains, M_{ij} is the diad molecular weight, and f_i is the mer fraction of species i. Regardless of the length distribution of dissolved hard segments, the mer fractions are dictated by stoichiometry to have the values

$$f_s = \frac{1}{2n+2}, \quad f_d = \frac{n+1}{2n+2}, \quad f_c = \frac{n}{2n+2} \tag{6}$$

where n is the average number of diisocyanate residues per dissolved hard segment. With these substitutions, the Couchman equations for a segmented polyurethane block copolymer become

$$\Delta C_{p_{dc}} = \frac{M_{sd} \Delta C_{p_{sd}} (T_g - T_{g_{sd}}) T_{g_{dc}}}{M_{dc} n (T_{g_{dc}} - T_g) T_{g_{sd}}} \tag{7}$$

and

$$W_1 = \frac{\Delta C_p (M_{sd} + n M_{dc})}{M_{sd} \Delta C_{p_{sd}} + n M_{dc} \Delta C_{p_{dc}}} \tag{8}$$

The principle unknowns in these equations are W_1, $\Delta C_{p_{dc}}$, and n. In general, they may be determined from the results of the DSC analysis alone. In the case of MDI-based polyurethanes, however, $\Delta C_{p_{dc}}$ is also an unknown because of the difficulty in observing a well-defined hard-segment glass transition process. The two equations (eqs 7 and 8) thus contain three unknowns, n, $\Delta C_{p_{dc}}$, and W_1; two knowns, M_{sd} and M_{dc}; and five measurable quantities, T_g, ΔC_p, $T_{g_{dc}}$, $T_{g_{sd}}$, and $\Delta C_{p_{sd}}$. The quantities T_g and ΔC_p are those values measured for the soft microphase of the copolymer of interest; $T_{g_{dc}}$ is measured from a pure hard-segment copolymer; and $T_{g_{sd}}$ and $\Delta C_{p_{sd}}$ are measured from a diisocyanate end-capped prepolymer or alternating diisocyanate/soft-segment copolymer. It is apparent that, in addition to (7) and (8), a third relationship is needed to solve for the three unknowns (i.e., n, $\Delta C_{p_{dc}}$, and W_1). This additional equation is furnished by relations obtained from small-angle X-ray scattering analysis described in the preceding paper. From this analysis the compositions and overall fractions of both the soft and hard microphases may be evaluated. (See Appendix A for a complete description of the method.)

A semiempirical approach can be developed as an alternative to the Couchman equations, as has been described in a previous publication.[5] The basis of the approach consists of two equations relating heat capacity changes, microphase compositions, and glass transition temperatures. For a homogeneous single-phase copolymer the total $\Delta C_{p_{mix}}$ is taken as the linear weighted combination of the two pure constituent values (i.e., soft segment denoted by 1 and hard segment by 2)[17]

$$\Delta C_{p_{mix}} = w_1 \Delta C_{p_1} + (1 - w_1) \Delta C_{p_2} \tag{9}$$

where w_i is the weight fraction of constituent i with heat capacity change ΔC_{p_i}. The T_g behavior for the mixture is

represented by a generalized Fox equation (15)

$$\frac{w_1 + (1-w_1)k}{T_{g_{mix}}} = \frac{w_1}{T_{g_1}} + \frac{k(1-w_1)}{T_{g_2}} \quad (10)$$

The parameters in (9) and (10) were obtained previously by experimental determination of $\Delta C_{p_{mix}}$ and $T_{g_{mix}}$ on quench-mixed specimens of various known compositions.[5] The previous analysis furnished values of $\Delta C_{p_1} = 0.194$ cal/g, $\Delta C_{p_2} \simeq 0$, $k = 1.18$, $T_{g_1} = -69$ °C, and $T_{g_2} = 109$ °C. In practice, the specimens are two-phase in nature; therefore, (9) and (10) are applied to characterize the composition of the soft microphase. That is, the fraction of soft segment in the soft microphase, $w_{1,s}$, is estimated by solving (10) for $w_1 = w_{1,s}$ with $T_{g_{mix}}$ replaced by the experimental soft microphase T_g and the additional parameters k, T_{g_1}, and T_{g_2} as given above. In principal, the soft-segment content of the hard microphase, $w_{2,s}$, could be determined by application of (10) to the hard microphase T_g. It is more consistent, however, to employ the lever rule, from which it follows that

$$w_{2,s} = \frac{W_{ss} - W_1 w_{1,s}}{(1 - W_1)} \quad (11)$$

where W_{ss} is the overall soft-segment weight fraction of the specimen. The overall weight fraction of the soft-segment-rich microphase is calculated from

$$W_1 = \frac{\Delta C_{p_s}}{\Delta C_{p_1} w_{1,s} + \Delta C_{p_2}(1 - w_{1,s})} \quad (12)$$

where ΔC_{p_s} is the measured heat capacity change at the soft microphase T_g. The previously determined pure component ΔC_p values are employed in (12) for this purpose. Details regarding the empirical calculation are presented in Appendix B.

Small-Angle X-ray Scattering Analysis. Small-angle X-ray scattering originates from spatial fluctuations in electron density within a material. Analysis of the SAXS intensity then can be used to estimate microphase compositions. The degree of microphase separation is characterized by the mean-squared variance in electron density, $\overline{\Delta\rho^2}$, which may be estimated by determination of the scattering invariant. Experimental invariants may be calculated following the method of Bonart et al.[20] The first invariant includes the effects of interfacial mixing and is given by

$$\overline{\Delta\rho^2}' = C\int_0^\infty [I(s) - \tilde{I}_b(s)]\, s\, ds \quad (13)$$

The second invariant corrects for the presence of diffuse microphase boundaries and is calculated from

$$\overline{\Delta\rho^2}'' = \frac{C\int_0^\infty [\tilde{I}(s) - \tilde{I}_b(s)]\, s\, ds}{\exp[-38(\sigma s)^{1.81}]} \quad (14)$$

The origins of these relations have already been discussed in detail.[1,4,20] $\tilde{I}(s)$ refers to the slit smeared scattered intensity; s is the scattering vector ($s = 2 \sin\theta/\lambda$, where 2θ is the scattering angle and λ is the wavelength); C is a known constant; $\tilde{I}_b(s)$ is a background intensity arising from thermal density and concentration fluctuations within the microphases; and σ is a parameter related to the diffuse microphase boundary thickness. The latter two terms are determined from regression to a modified Porod relation.[21,22]

The relationship between the SAXS variances (eqs 13 and 14) and phase compositions follows from the general definition of a second moment of the electron density distribution for a two-phase system

$$\overline{\Delta\rho^2} = \phi_1(\rho_1 - \bar{\rho})^2 + (1 - \phi_1)(\rho_2 - \bar{\rho})^2 \quad (15)$$

The material average electron density is defined as

$$\bar{\rho} = \phi_1\rho_1 + (1 - \phi_1)\rho_2 \quad (16)$$

where ρ_1 and ρ_2 are the average electron densities of the soft and hard microphases, respectively.

The material average electron density may be evaluated from the known chemical composition of the material and an experimental measurement of its mass density.[23] The system of SAXS relations effectively consists of two equations with two measurable quantities, $\overline{\Delta\rho^2}$ and $\bar{\rho}$, and three unknowns. The additional information needed to solve the complete system of equations is furnished by one of the DSC analyses described in the preceding section. The complete set of equations is quite cumbersome due to the involvement of volume fractions, mass fractions, mass densities, and electron densities and is described in detail in the appendices. Solution of these equations yields a complete specification of the amounts and compositions of each microphase.

Table I
Specimen Characteristics

material	hard segment (wt %) (MDI + BDO)	density (g/cm³)	av MW[a] of hard segment (g/mol of HS)	no. of MDI per hard segment[a]
PU-20	20	1.142	500	1.7
PU-30	30	1.165	900	2.8
PU-40	40	1.192	1400	4.2
PU-50	50	1.218	2000	6.2
PU-60	60	1.235	3100	9.2
PU-70	70	1.270	4800	14.1
PU-80	80	1.292	8100	24.0

[a] Calculated from Peeble's most probable distribution for one-step polymerization.[3]

III. Experimental Section

Materials. A series of segmented polyurethane block copolymers with varying hard-segment content are studied. The hard segments consist of a 4,4′-diphenylmethane diisocyanate (MDI) chain extended with 1,4-butanediol (BDO). The soft segment is poly(oxpropylene) (PPO, $M_n = 2000$, functionality = 1.94) end-capped with 30.4 wt % poly(oxyethylene) (PEO). The polymers are prepared by a one-step bulk polymerization process with 4% excess MDI to ensure complete reaction (eq 13). The notation used for this series of polymers is PU-XX, where XX represents the weight fraction of the hard segment. The chemical compositions of the materials studied are presented in Table I along with some associated physical characteristics. The polymers used in this study[1,2,5,13] are reprecipitated from dimethylformamide solutions of the as-received polymers and then molded into 2-mm-thick, 1.5-in.-diameter disks at 180 °C and 3000 psi for 5 min under vacuum. Elemental analysis of a few selected samples confirms that the as-molded polymers have the same chemical content as the original samples. These molding conditions were selected since they produced materials that present only a single melting endotherm in high-rate DSC tests (see first paper in this series). The materials should therefore possess morphologies which are uniform across an entire specimen.

The pure alternating block copolymer of MDI and the soft segment (denoted PU-MDI) is prepared by solution polymerization in tetrahydrofuran (THF). THF is dried under calcium hydride and distilled over sodium wire and benzophenone prior to usage. The MDI (Eastman Kodak) is filtered through a fritted-glass filter at 80 °C in order to remove dimers and impurities. The MDI monomers are added slowly to the reacting solution (5% solution in THF) at 10% in excess of the stoichiometric ratio. Less than 1% of dibutyltin dilaurate (DBTL) is used as

Table II
Results of Experimental Characterization

material	ΔC_{p_s} (cal/g K) at soft microphase T_g	T_{g_s} (K) of soft microphase	T_{g_h} (K) of hard microphase	electron density variances [(mol e/cm^3)^2 × 10^{-3}] $\overline{\Delta\rho^{2'}}$	$\overline{\Delta\rho^{2''}}$
polyol	0.198	204			
prepolymer	0.168	215			
PU-30	0.132	233	364	0.525	0.625
PU-40	0.119	230	356	0.625	0.792
PU-50	0.092	230	353	0.972	1.080
PU-60	0.0635	232	351	1.030	1.170
PU-70	0.038	239	346	0.974	1.110

a catalyst for the reaction. The reaction is carried out at 60 °C and rigorously stirred for 2 days to complete the reaction. The polymer is then reprecipitated from solution with dried methanol.

Small-Angle X-ray Scattering. Small-angle X-ray scattering experiments are performed on a step-scanning Kratky camera equipped with a proportional counter (Cu Kα source with a Ni filter, wavelength $\lambda = 1.5418$ Å). The sample-to-detector distance is 214 mm and the step size between each measurement is 50 μm. A Lupolen standard is used for the purpose of absolute intensity calibration. The raw intensity curves are then smoothed,[1] corrected for parasitic slit scattering and sample attenuation, and desmeared according to Vonk's routine.[14] A more complete description of the analysis procedure is given in the preceding paper.

IV. Results

Microphase Composition Calculations. Extension of Couchman's Theory. Calculation of the microphase composition by coupling the SAXS invariant data with the modified Couchman relations for the case of segmented polyurethanes is described fully in the Appendix A. In order to solve these equations, a number of parameters need to be determined experimentally. The specific volume of the pure soft segment is measured pycnometrically,[23] and that of the pure hard segment is obtained from the total polymer density (measured by the buoyancy method) by assuming volume additivity.[1] ΔC_p and T_g of the soft microphase were measured by DSC in the preceding paper, as were $\Delta C_{p_{sd}}$ and $T_{g_{sd}}$ (from the end-capped prepolymer) (see Table II). The other parameters in the relations are fixed except for $T_{g_{dc}}$ and $\Delta C_{p_{dc}}$, for the pure hard segment. Fixing either of these parameters is sufficient to solve the equations. In order to simplify the equations, we assume a value of $T_{g_{dc}} = 110$ °C, as has been reported in the literature.[8] We also assume that $T_{g_{dc}}$ is a constant, independent of the sequence length distribution (i.e., molecular weight of the dissolved hard segments), although there is some evidence that it is influenced by molecular weight.[24] Finally, we neglect the crystallinity of the hard microdomain, which has been estimated at less than 23% for all materials (see preceding paper). The parameters which we will solve for are n, the average length of hard segment dissolved within the soft microphase, $\Delta C_{p_{dc}}$, and W_1, the overall weight fraction of the soft microphase. From these parameters, all other parameters may then be calculated. An iterative procedure is adopted for the solution of these relations. First, a value of n is assumed, whereupon a value for the theoretical X-ray invariant $\overline{\Delta\rho_T^{2''}}$ is calculated (A.14). The value of n is then adjusted in iterative fashion until the theoretical invariant is equal to one of the two experimental invariants $\overline{\Delta\rho^{2'}}$ and $\overline{\Delta\rho^{2''}}$ (see Table II).

The two experimental invariants lead to different results because they treat the interphase material differently. Which value is appropriate depends upon whether or not the interfacial material contributes to the soft microphase glass transition process. In the first model (lower part of Figure 1), it is apparent that $\overline{\Delta\rho^{2'}}$ incorporates mixing

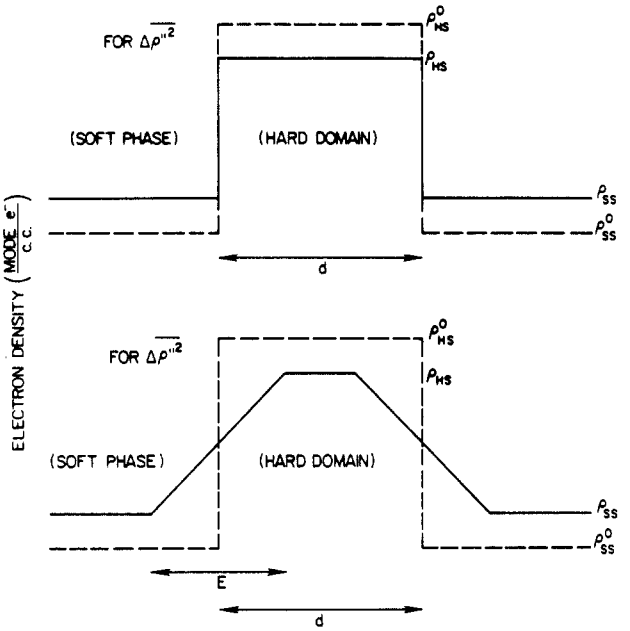

Figure 1. Hypothetical electron density profiles for pseudo-two-phase systems. The dashed profiles denote a system which is completely segregated. The solid profile in the upper figure represents a system which comprises intermixed microphases resulting in an electron density variance $\overline{\Delta\rho^{2''}}$. The lower solid profile with electron density variance $\overline{\Delta\rho^{2'}}$ shows the case where mixing occurs both within the microphases and at the microphase boundary.

both at the interphase and within the bulk microphase. Calculations based upon this invariant therefore include the interphase material in the T_g modeling and will give an upper bound on the degree of mixing. The invariant $\overline{\Delta\rho^{2''}}$ corresponding to the model in the upper half of Figure 1 is corrected for the interphase material. The T_g modeling does not consider interfacial material and thus represents a lower bound on the degree of mixing.

The results of calculations based upon the two invariant models are given in Tables III and IV, respectively. Neither model produces satisfying results. The value of n, for example, does not exhibit behavior consistent with our previous SAXS modeling[1,4] and the results of the preceding paper. In this model, we propose the existence of a critical hard-segment length. All segments below this critical length would dissolve in the soft microphase. The value of n obtained, however, is not approximately constant as would be expected from this reasoning. In addition, the $\Delta C_{p_{dc}}$ values are not reasonable, especially for the results based upon $\overline{\Delta\rho^{2'}}$. In this case, $\Delta C_{p_{dc}}$ exceeds that of the pure soft segment (0.1976 cal/g °C) for all cases. The best estimate of $\Delta C_{p_{dc}}$ determined from the reported $T_{g_{dc}}$ and the Simha–Boyer rule[25] is only 0.07 cal/g °C. The $\Delta C_{p_{dc}}$ results based upon $\overline{\Delta\rho^{2''}}$ (Table III) show a minimum value of 0.13 cal/g °C for PU-50, in reasonable agreement with the prediction of the Simha–Boyer rule.

Table III
Microphase Composition Calculations Based upon $\overline{\Delta\rho^2}'$, Including Interphase Material[a]

sample	av no. of BDO, n	$\Delta C_{p_{dc}}$	wt fraction soft phase, W_1	vol fraction soft phase, ϕ_1	wt fraction HS in soft phase $W_{1,h}$	SS in soft phase $\phi_{1,s}$	HS in hard phase $\phi_{2,h}$
PU-30	0.20	0.6712	0.6712	0.6920	0.1373	0.8854	0.5561
PU-40	1.51	0.7458	0.7458	0.7658	0.2760	0.7634	0.7705
PU-50	1.63	0.5895	0.5895	0.6173	0.2882	0.7539	0.8188
PU-60	0.64	0.3516	0.3516	0.3804	0.1891	0.8406	0.7491
PU-70	0.44	0.1959	0.1959	0.2190	0.1667	0.8601	0.8214

[a] The invarants used are corrected for thermal density fluctuations and employ the parameters $T_{g_{dc}}$ = 110 °C, $T_{g_{sd}}$ = −57.6 °C, $\Delta C_{p_{sd}}$ = 0.1679 cal/g °C, hard segment density = 1.354 g/cm³, and soft segment density = 1.01 g/cm³.

Table IV
Microphase Composition Calculations Based upon $\overline{\Delta\rho^2}''$, Excluding Interphase Material[a]

sample	av no. of BDO, n	$\Delta C_{p_{dc}}$	wt fraction soft phase, W_1	vol fraction soft phase, ϕ_1	wt fraction HS in soft phase, $W_{1,h}$	SS in oft phase, $\phi_{1,s}$	HS in hard phase $\phi_{2,h}$
PU-30	0.05	4.97	0.6560	0.6789	0.1173	0.9025	0.5750
PU-40	1.35	0.14	0.7312	0.7529	0.2614	0.7765	0.7821
PU-50	0.38	0.13	0.5721	0.6016	0.2648	0.7735	0.8259
PU-60	0.26	0.82	0.3335	0.3639	0.1451	0.8787	0.7563
PU-70	(0.00)	5.00	0.1837	0.2075	0.1112	0.9077	0.8241

[a] The invariants used are corrected for thermal density fluctuations and diffuse boundary thickness and employ the parameters $T_{g_{dc}}$ = 110 °C, $T_{g_{sd}}$ = −57.6 °C, $\Delta C_{p_{sd}}$ = 0.1679 cal/g °C, hard segment density = 1.354 g/cm³, and soft segment density = 1.01 g/cm³.

Table V
Microphase Composition Calculations Based upon the Modified Fox Empirical Model

sample	volume fraction soft phase, ϕ_1	SS in soft phase, $W_{1,s}$	HS in hard phase, $W_{2,h}$	fraction of HS dissolved in soft phase	apparent T_g (K) hard phase	electron density variance
PU-30	0.893	0.764	0.836	0.703	340	0.43
PU-40	0.779	0.786	(1.06) 1.00[a]	0.416	(400) 382[a]	1.54
PU-50	0.599	0.790	0.934	0.251	364	1.58
PU-60	0.424	0.771	0.874	0.162	349	1.27
PU-70	0.270	0.720	0.856	0.108	344	0.82

[a] Assuming a pure hard phase.

Unreasonably high values are seen for compositions at the two limits however. As a consequence of the $\Delta C_{p_{dc}}$ behavior, the predicted soft-segment contents for both models show a minimum for PU-50. This is contrary to the overall trend observed in the experimental T_g data for the soft phase (Table II). The predicted hard-segment fractions of the hard phase show a maximum as a function of the hard-segment content, whereas the experimental apparent hard microdomain glass transition temperatures (Table II) decrease monotonically with an increase in the hard-segment content.

It is evident from these calculations that the extended Couchman theory does not account for the glass transition behavior in polyurethane elastomers. This in part can be attributed to the observation that the heat capacity change of the dissolved hard segments at the soft microphase T_g is effectively zero.[2,5,9] In addition, other physiochemical phenomena may occur that can effect the T_g process. It is probable, for example, that the dissolved hard segments participate in hydrogen bonds either with other dissolved hard segments or with the ether oxygen of the soft segment.[26] Sung and Schneider[27] have postulated that hydrogen bonds can influence the T_g process through their role as physical cross-links. In addition, as was mentioned previously, we have assumed that $T_{g_{dc}}$ is independent of sequence length, whereas there is some indication[24] that the chemical junctions between blocks act in much the same fashion as end groups to impart a sequence length dependence to $T_{g_{dc}}$. Finally, there is some ambiguity as to how to treat the material in the interphase region. We have no clear idea of how much of the interfacial material takes part in the soft microphase glass transition process. Since our estimates indicate that the interphase in polyurethanes may account for as much as 20% of the material,[28] this ambiguity can lead to substantial error. At present, it appears unlikely that a rigorous approach including all of the factors which influence the T_g's of these polyurethanes can be developed. The approach developed herein or a similar one may be useful in examining the behavior of less complicated segmented copolymers.

A Self-Consistent Phenomenological Approach. In view of the deficiency of the straightforward thermodynamic approach to modeling polyurethanes, there is considerable motivation to develop a more empirical approach to the problem of determining microphase compositions. Such an approach readily presents itself as a result of the accessability of the homogeneous (i.e., disordered) state for polyurethanes. It has been previously demonstrated[5] that at temperatures of ca. 240 °C, microphase separation is not manifest. Furthermore, the disordered, mixed state may be frozen in by rapidly quenching these materials. The T_g and ΔC_p behavior of these quenched samples can serve as a calibration for the effect of mixture composition on the T_g and ΔC_p of either the hard or soft phase. This calibration would presumably account for all effects, such as molecular length, mixing, and hydrogen bonding, which influence the glass transition temperature. Previously,[5] we found that the ΔC_p behavior of our materials quenched from the disordered state followed (9), yielding regression parameters of ΔC_{p_1} = 0.194, equivalent to that measured for the pure soft segment (i.e., 0.198), and $\Delta C_{p_2} \approx 0$.

The behavior of the single T_g observed for the disordered quenched specimens was found to be well described by the modified Fox equation (eq 10), with T_{g_1} = 213 K measured from the pure soft segment, T_{g_2} = 383 K, and k = 1.18 determined by regression of (10) upon the experimental T_g vs W_1 data. Equations 9 and 10 then serve as semiempirical calibration relations which may be

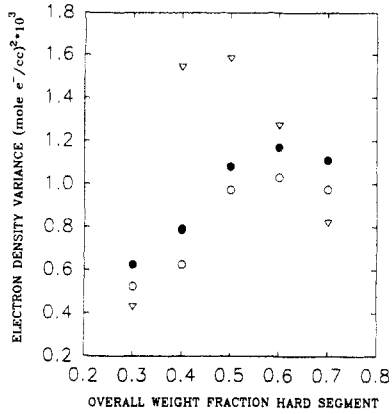

Figure 2. Comparison of the measured electron density variances, $\overline{\Delta\rho^2}''$ (filled circles) and $\overline{\Delta\rho^2}'$ (open circles) with predictions from the self-consistent phenomenological model (triangles).

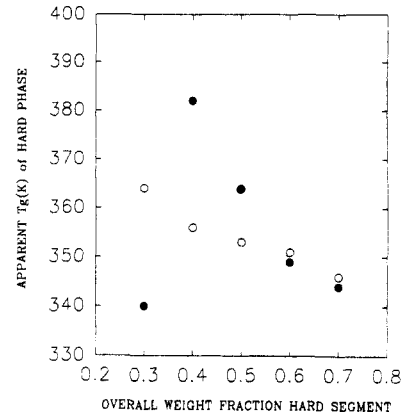

Figure 3. Apparent hard microphase glass transition temperatures. Open circles refer to the results of DSC measurements; filled circles denote predictions from the self-consistent phenomenological model.

applied to characterize either the hard or soft microphase compositions through analysis of the respective ΔC_p and T_g for that microphase. The use of this phenomenological approach allows one to take into account the actual T_g behavior even though the fundamental principles underlying this behavior may not be clearly understood. The self-consistency of the approach may be examined in two ways: by calculation of a theoretical invariant and comparison to experimental results and by calculation of the hard microphase T_g's and comparison to experimental results.

The self-consistent calculation begins by application of (10) to the experimental soft microphase T_g data. This leads to the composition of the soft microphase. The overall weight fraction of the soft microphase is determined by application of (9) to the ΔC_p data for the soft microphase glass transition. At this point the compositions and volume fractions of both microphases are known. A theoretical estimate of the invariant may then be obtained through relations (A.11–A.14) and appropriate transformations between weight and volume fractions. A theoretical estimate of the hard microphase T_g is then provided by application of (10) to the hard-segment-rich mixture. (See Appendix B for details of the calculation).

The results of the self-consistent empirical model calculations are given in Table V. Qualitatively, the results are pleasing. The purity of the phases, reflected in the values of the third and fourth columns of Table V is lowest for low and high contents of hard segment and goes through a maximum at intermediate hard-segment contents.

A more quantitative comparison of the model with experimental data is presented in Figures 2 and 3. The calculated electron density variances (Figure 2) reflect the same qualitative trend as both of the experimentally determined variances (see eqs 13 and 14). The agreement is good for low and high hard-segment contents; however, the calculation overestimates the variance at intermediate compositions. A similar trend is observed when comparing the apparent hard microphase glass transition temperatures in Figure 3. The T_g is overestimated at intermediate compositions corresponding to an overestimate in hard microphase purity. This result is consistent with the overestimate in the electron density variance for the same compositions.

In light of the many assumptions that have gone into the empirical model, the qualitative agreement with experiment is promising. Several of these assumptions warrant further examination. First of all, the effects of crystallization have been neglected. While the materials have been processed to give low crystallinities (i.e., less than 23%), the presence of crystallinity is a complicating

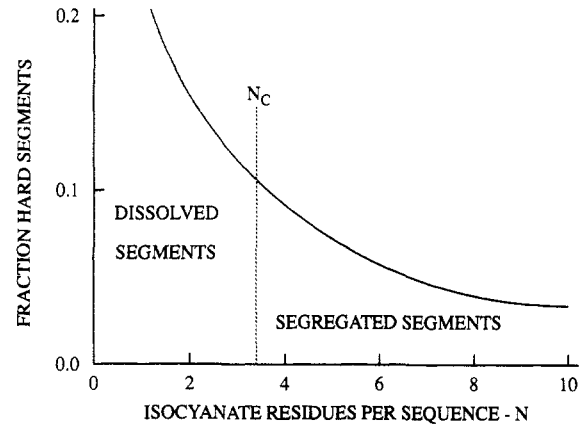

Figure 4. Schematic representation of the hard-segment length distribution function (number average) illustrating the role of the critical sequence length, N_c.

factor and leads to several important questions. Would it be more appropriate to employ a three-phase model consisting of a crystalline hard segment, a mixed hard phase, and a mixed soft phase? Where is the mixed hard phase located; is it truly a separate phase? How will crystallinity affect the apparent hard phase T_g? In fact, the variance data in Figure 2 are consistent with the degree of crystallinity data discussed in the first paper of this series. These data showed a gradual increase in crystallinity up to a maximum of ca. 22% for PU-70.

Second, the hard-segment glass transition temperature has been assumed to be independent of molecular weight. A limited amount of experimental data suggest the contrary is true.[24] Incorporation of a molecular weight dependent T_g into the theory would be an involved task due to the intrinsic distribution in molecular weight of the hard segment. In practice, two molecular weight distributions would be required, one for the dissolved hard segments and another for the segregated hard segments. Each population would have a distinct T_g. The calibration of T_g based upon specimens frozen in the disordered state by quenching only gives information regarding T_g of the entire hard-segment length distribution.

It is clear that, to better test the models we have developed, it would be appropriate to apply them to a simpler polyurethane system which is incapable of crystallization. Our initial attempts at this approach have failed due to the strong tendency for noncrystallizable urethanes to absorb water and consequently degrade during processing. Efforts to circumvent this problem are ongoing and should result in a better test of these equations for the determination of microphase composi-

Table VI
Estimated Critical Hard-Segment Sequence Lengths[a]

material	N_c		
	$x = 1$	$x = 0.99$	$x = 0.95$
PU-30	5.5	5.4	5.0
PU-40	5.2	5.1	4.8
PU-50	5.4	5.3	5.0
PU-60	6.1	6.0	5.7
PU-70	7.3	7.3	6.9

[a] Hard segments with N_c or more diisocyanate residues per sequence length are assumed to reside within the hard microdomain; x is the fractional conversion.

tions in polyurethanes and other segmented block copolymers.

Comparison with the Koberstein–Stein Model of Polyurethane Microdomain Structure. The Koberstein–Stein model of microdomain structure[4] is based upon the concept of a critical hard-segment sequence length. Hard-segment sequences shorter than this length are thought to dissolve within the soft microphase. Sequences longer than the critical length segregate into hard microdomains with a more or less lamellar structure and a thickness roughly equivalent to the critical sequence length. If the hard-segment sequence length follows a most probable distribution as expected,[3] the partitioning of hard-segment species between the soft and hard microphases would most likely occur as depicted schematically in Figure 4. Since polyurethanes of varying hard-segment content will have intrinsically different hard-segment distributions, they will also contain different amounts of intersegmental mixing. The critical hard-segment sequence length however should depend primarily on the soft-segment type and length and be relatively independent of hard-segment content.

The preceding paper in this series and earlier papers from our laboratory have examined many of the features of this model and found them to be consistent with a variety of experimental data. A further comparison can be made through examination of the microphase composition data from the present analysis. Since all microphase compositions are known (within the assumptions and validity limits of the analysis), the fraction of hard segments dissolved within the soft microphase can be determined by

$$W_{h,dissolved} = \frac{W_1 w_{1,h}}{W_1 w_{1,h} + (1 - W_1) w_{2,h}} \quad (17)$$

The critical sequence length, N_c, can be evaluated by integrating the sequence length distribution until $W_{h,dissolved}$ equals the fraction of sequences below the critical length.

The estimated fractions of hard segments dissolved within the soft microphase are given in Table V based upon the empirical model calculation. The critical hard-segment sequence lengths calculated from this data (using distributions derived by Peebles[3]) are given in Table VI. The critical lengths are sensitive to the degree of reaction conversion assumed in the calculation of the hard-segment sequence length distribution. The critical length increases with an increase in conversion.

An estimate of the conversion may be obtained by consideration of the overall molecular weight of the polymers. The number-average molecular weight of PU-60 (estimated from gel permeation chromatography relative to polystyrene standards) is about 50 000. This corresponds to a conversion of about 99%. Assuming 99% conversion, the calculated critical lengths are approximately 5–6, indicating that hard-segment sequences containing 5–6 or more diisocyanate residues are segregated to form the hard microdomain. This result is consistent with the idea of a critical length as embodied in the Koberstein–Stein model, although it is difficult to ascertain an absolute value without direct knowledge of the hard-segment sequence length distribution. A value of 3–4 was obtained from SAXS analysis in the preceding paper.

Table VII
Calculated Hard Microdomain and Repeat Unit Thickness

material	vol fraction hard microdomain, ϕ_2	SAXS interdomain spacing, d_{1D} (nm)	hard microdomain thickness, T_{HS} (nm)	repeat unit thickness (nm), T_{HS}/N_c (99% convn)
PU-30	0.299	15.2	4.5	0.83
PU-40	0.584	21.9	12.8	2.5
PU-50	0.743	13.7	10.2	1.9
PU-60	0.838	13.3	11.1	1.85
PU-70	0.891	11.7	10.4	1.4

The thickness of the hard microdomain, assuming a lamellar morphology, can be calculated from

$$T_{HS} = \phi_2 d_{1D} \quad (18)$$

where ϕ is the volume fraction of the hard microphase (determined from the modified Fox model), and d_{1D} is the one-dimensional interdomain period determined by small-angle X-ray scattering (see the preceding paper). These values are presented in Table VII. Except for PU-30, for which the lamellar assumption in (17) is probably inappropriate, the hard-segment thickness is roughly constant, falling in the range of 10–13 nm. These data are also consistent with the Koberstein–Stein model of polyurethane morphology which predicts that the critical hard-segment length controls the thickness of the hard microdomain. Our estimated value of N_c is ca. 5–6 for specimens of hard-segment contents of 40% and higher, suggesting a constant microdomain thickness in these materials.

These findings are contrary to the behavior reported for monodisperse hard-segment model compounds,[29] where the crystal thickness is linearly dependent on the sequence length. It is interesting to note however that our estimated repeat unit lengths (i.e., the microdomain thickness divided by N_c) fall in the range of 1.4–2.5 nm (see Table VII), which compare well with the value of ca. 1.9–2.0 nm reported for the d_{001} spacing of the hard-segment model compounds.

From these results, it appears that the morphological behavior of polyurethanes is strongly dependent on polydispersity. In monodisperse model compounds, extended chains predominate, while in normal segmented polyurethanes with continuous hard microdomains, the evidence supports the occurrence of some type of hard-segment chain folding/coiling or reentry into the hard microdomain. This need not be tight folds with adjacent reentry as considered in the model compound studies and would probably result in a highly disordered structure commensurate with the poorly defined diffraction patterns observed for bulk polyurethanes.

V. Conclusions

Two methods have been developed and evaluated for the determination of microphase compositions in segmented block polyurethanes. The first method, a rigorous thermodynamic treatment combining an extension of Couchman's theory applied to glass transition data with small-angle X-ray scattering analyses, fails to yield self-consistent microphase compositions. We conclude from this result that the glass transition behavior of polyurethanes is more complex than can be accounted for by strictly thermodynamic treatments such as that of Couch-

man. Additional phenomena that need to be considered include the effects of hydrogen bonding and the associated physical cross-linking, and the dependence of the glass transition on the hard-segment sequence length distribution. Furthermore, the effect of the interfacial material on the glass transition is not well understood.

A second, self-consistent phenomenological approach is found to be reasonablly successful in calculating microphase compositions. This approach uses samples which have been quenched into the disordered state to calibrate a modified Fox equation for the glass transition behavior of mixed microphases. The results of these calculations show trends which are consistent with SAXS and T_g behavior: the overall degree of microphase separation shows a maximum for samples where the volume fractions of hard and soft segments are roughly equal; the glass transition temperature of the hard microphase decreases more or less monotonically with hard-segment content, indicating an associated increase in the soft-segment content of the hard microphase; the T_g of the soft microphase increases with an increase in the hard-segment content, indicating increasing hard segment within the soft microphase.

The SAXS data are also consistent with the Koberstein–Stein model for the microdomain structure of polyurethanes. The microdomain thickness is essentially constant, indicating a folded/coiled chain lamellar morphology. The critical hard-segment sequence length is estimated to contain ca. 5–6 MDI residues. Sequences shorter than this critical length remain within the soft microphase and account for the observed elevation in the soft microphase T_g.

Several assumptions inherent to the modeling warrant further investigation with model systems. Crystallinity, for example, was not taken into account but may influence our results. Examination of a noncrystalline polyurethane would be a valuable simplification. Finally, the dependence of T_g on the sequence length requires a thorough investigation, as the sequence length distribution can change markedly from one formulation to another.

The understanding of these fundamental aspects of polyurethane morphology is essential in the attainment of the goal of designing the properties of these complex, yet versatile, materials. Models such as those presented herein must certainly be refined to be more quantitative but already provide a valuable framework for qualitative prediction of structure–property relationships for polyurethane copolymers.

Acknowledgment. We thank Dr. R. Zdrahala, formerly of Union Carbide Corp., for supplying the samples and Dr. J. A. Emerson for use of the Western Electric SAXS facility in Princeton, NJ. This work was supported by grants from the Polymers Section of the National Science Foundation, Division of Materials Research (DMR-8105612), and the Office of Naval Research.

Appendix A. Calculation of Microphase Compositions Using Couchman's Theory Combined with SAXS Analysis

The small-angle X-ray scattering invariant calculation (eqs 13 and 14) provides an estimate of the mean-squared fluctuation in electron density or electron density variance. By definition, for a two-phase system, the variance is related to the volume fraction ϕ_i and electron densities ρ_i of the microphases

$$\overline{\Delta\rho}^2 = \phi_1(\rho_1 - \bar{\rho})^2 + (1 - \phi_1)(\rho_2 - \bar{\rho})^2 \qquad (A.1)$$

1 and 2 refer to the soft and hard microphases, respectively. The material average electron density is defined as

$$\bar{\rho} = \phi_1\rho_1 + (1 - \phi_1)\rho_2 \qquad (A.2)$$

If the two microphases are each mixtures of hard and soft segments, their electron densities may be written

$$\rho_1 = \phi_{1,s}\rho_s + (1 - \phi_{1,s})\rho_h \qquad (A.3)$$

and

$$\rho_2 = \phi_{2,s}\rho_s + (1 - \phi_{2,s})\rho_h \qquad (A.4)$$

where the subscript s and h refer to the soft and hard segments, respectively. The term $\phi_{1,s}$, for example, is the volume fraction of soft segment in phase 1, that is, the soft microphase.

The set of SAXS equations contains five unknowns: ϕ_1, ρ_1, ρ_2, $\phi_{1,s}$, and $\phi_{2,s}$. The variance $\overline{\Delta\rho}^2$ is measured experimentally; ρ_s is determined from the measured mass density and known chemical composition of the pure soft segment; $\bar{\rho}$ is calculated from the measured mass density and known chemical composition of the block copolymer; ρ_h is calculated from the known overall hard-segment content, ϕ_h, with the assumption of volume additivity

$$\rho_h = \frac{\bar{\rho} - (1 - \phi_h)\rho_s}{\phi_h} \qquad (A.5)$$

In order to solve the four equations with five unknowns, additional equations are obtained from the DSC analysis of the soft microphase. In constructing these equations, the equations of Couchman are modified[11,17,18] to accommodate the polyurethane structure. This structure may be represented as $-[(dc)_n ds]-$ for all hard-segment sequences which are dissolved within the soft microphase where n is the average length of a dissolved hard segment, s is a soft segment, d a diisocyanate residue, and c a chain extender residue. It follows that the number fraction of the species are

$$f_s = \frac{1}{2n+2}, \quad f_d = \frac{n+1}{2n+2}, \quad f_c = \frac{n}{2n+2} \qquad (A.6)$$

As a result of the alternating structure of the chain, only two diads are possible, a hard/soft-segment moiety (sd) and a hard segment/chain extender diad (dc). From the known molecular weights (s = 2000, d = 250, and c = 90) the diad weight fractions following (5) become

$$f_{sd} = \frac{(n+1)(2250)}{M} \text{ and } f_{dc} = \frac{n(n+1)(340)}{M} \qquad (A.7)$$

Substitution into (7) and (8) gives

$$\Delta C_{p_{dc}} = \frac{2250\Delta C_{p_{sd}}(T_g - T_{g_{sd}})T_{g_{dc}}}{340n(T_{g_{dc}} - T_g)T_{g_{sd}}} \qquad (A.8)$$

and

$$W_1 = \frac{\Delta C_p(2250 + 340n)}{2250\Delta C_{p_{sd}} + 340n\Delta C_{p_{dc}}} \qquad (A.9)$$

The unknowns in these two equations are $\Delta C_{p_{dc}}$, W_1, and n. $T_{g_{dc}}$ is taken from the literature as 110 °C,[8] and $\Delta C_{p_{sd}}$ and $T_{g_{sd}}$ are the measured values for PU-MDI; T_g and ΔC_p are experimental values determined for the copolymer of interest. In order to solve for the three unknowns in (A.8) and (A.9), additional equations are required that relate to the SAXS equations (eqs A.1–A.4).

A solution is determined by iteration. After assuming a value for n, $\Delta C_{p_{dc}}$ is calculated from (A.8), and subsequently W_1 may be determined from (A.9). With $\Delta C_{p_{dc}}$

and W_1 known, and n assumed, a theoretical SAXS invariant can be evaluated from the following relations. The volume fraction of soft segment in the soft microphase is

$$\phi_{1,s} = \frac{f_s M_s \nu_s}{f_s M_s \nu_s + (f_d M_d + f_c M_c)\nu_h} = \frac{2000\nu_s}{2000\nu_s + (340n + 250)\nu_h} \quad \text{(A.10)}$$

where the f_i terms are defined in (6) and ν_i is the specific volume; ν_s for the pure soft segment is measured, and ν_h for the pure hard segment is estimated from ν_s and the specific volume of the copolymer of interest, ν_T, by assuming volume additivity.

The overall volume fraction of the soft-segment-rich microphase or soft microphase is then calculated from

$$\phi_1 = W_1/\{\nu_T[\phi_{1,s}/\nu_s + (1 - \phi_{1,s})/\nu_h]\} \quad \text{(A.11)}$$

The electron density of the soft microphase is calculated from

$$\rho_1 = \phi_{1,s}\rho_s + (1 - \phi_{1,s})\rho_h$$

where ρ_s and ρ_h are the electron densities of the pure soft segment and pure hard segment, respectively. ρ_s is measured from the pure soft segment and ρ_h is estimated from the measured material average electron density, $\bar{\rho}$, assuming volume additivity. The hard microphase electron density is determined by rearranging (16) to give

$$\rho_2 = \bar{\rho} - \phi_1\rho_1(1 - \phi_1) \quad \text{(A.12)}$$

The material average electron density is dictated by the reaction stoichiometry to be

$$\bar{\rho} = [W_{SS}\nu_s\rho_s + (1 - W_{SS})\nu_h\rho_h]/\nu_T \quad \text{(A.13)}$$

where W_{SS} is the overall weight fraction of the soft segment in the copolymer formulation.

A theoretical SAXS invariant is then calculated from

$$\overline{\Delta\rho_T}^{2'''} = \phi_h(1 - \phi_h)(\rho_h - \rho_s)^2 \quad \text{(A.14)}$$

The theoretical invariant thus calculated is then compared to the experimental invariants $\overline{\Delta\rho}^{2'}$ and $\overline{\Delta\rho}^{2''}$. The assumed value of n is then adjusted iteratively until the theoretical and experimental invariants agree. Attainment of this convergence furnishes complete specification of the microphase compositions and amounts.

Appendix B. Calculation of Microphase Compositions and Properties Using the Modified Fox Analysis

The overall weight fraction of the soft microphase (following eq 12) is given by

$$W_1 = \frac{\Delta C_{p_s}}{w_{1,s}\Delta C_{p_1} + \Delta C_{p_2}(1 - w_{1,s})} \quad \text{(B.1)}$$

A previous calibration of the polyurethanes used in this study yielded $\Delta C_{p_1} = 0.194$ and $\Delta C_{p_2} \simeq 0$. Thus the experimental measurement of the heat capacity change at the soft microphase T_g, ΔC_{p_s}, is sufficient to calculate W_1.

The composition of the soft microphase is determined by application of (10) to experimental measurements of T_{g_s}, the soft microphase T_g. The weight fraction of the soft segment in the soft microphase, $w_{1,s}$, is determined from

$$w_{1,s} = \frac{kT_{g_1}(T_{g_s} - T_{g_2})}{T_{g_2}(T_{g_1} - T_{g_s}) + kT_{g_1}(T_{g_s} - T_{g_2})} \quad \text{(B.2)}$$

The previous analysis furnished values of $k = 1.18$, $T_{g_1} = -69$ °C, and $T_{g_2} = 109$ °C. The composition of the hard microphase is then given by the lever rule

$$w_{2,s} = \frac{W_{SS} - W_1 w_{1,s}}{(1 - W_1)} \quad \text{(B.3)}$$

where W_{SS} is the known overall weight fraction of the soft segment in the material. The T_g of the mixed hard microphase can then be calculated by rearrangement of (10) to give

$$T_{g_h} = \frac{[w_{2,s} + (1 - w_{2,s})k]T_{g_1}T_{g_2}}{w_{2,s}T_2 + k(1 - w_{2,s})T_{g_1}} \quad \text{(B.4)}$$

Once the phase compositions are known, the electron variances are calculated by application of (A.11–A.14).

References and Notes

(1) Leung, L. M.; Koberstein, J. T. *J. Polym. Sci., Polym. Phys. Ed.* **1985**, *23*, 1883.
(2) Koberstein, J. T., Galambos, A. F., Leung, L. M. *Macromolecules*, preceding paper in this issue.
(3) Peebles, L. M., Jr. *Macromolecules* **1974**, *7*, 872; **1976**, *9*, 58.
(4) Koberstein, J. T.; Stein, R. S. *J. Polym. Sci., Polym. Phys. Ed.* **1983**, *21*, 1439.
(5) Leung, L. M.; Koberstein, J. T. *Macromolecules* **1986**, *19*, 706.
(6) Clough, S. B., Schneider, N. S. *J. Macromol. Sci., Phys.* **1968**, *B2* (4), 553.
(7) Schneider, N. S.; Sung, C. S. P. *Polym. Eng. Sci.* **1977**, *17*, 73.
(8) MacKnight, W. J.; Yang, M.; Kajiyama, T. *Polym. Prepr. (Am. Chem. Soc., Div. Polym. Chem.)* **1968**, *9*, 860.
(9) Camberlin, Y.; Pascault, J. P. *J. Polym. Sci., Chem.* **1983**, *21*, 415.
(10) Fox, T. G. *Bull. Am. Phys. Soc.* **1956**, *1*, 123.
(11) Couchman, P. R. *J. Mater. Sci.* **1980**, *15*, 1680.
(12) For a general discussion of these methods, see ref 1.
(13) Zdrahala, R. J.; Critchfield, F. E.; Gerkin, R. M.; Hager, S. L. *J. Elastomer Plast.* **1980**, *12*, 184.
(14) Vonk, C. G. *J. Appl. Crystallogr.* **1971**, *4*, 340.
(15) Wood, L. A. *J. Polym. Sci.* **1958**, *28*, 319.
(16) Gibbs, J. H.; Di Marzio, E. A. *J. Chem. Phys.* **1958**, *28*, 319.
(17) Couchman, P. R. *Macromolecules* **1978**, *11*, 117; **1980**, *13*, 1272.
(18) Couchman, P. R. *Nature* **1982**, *298*, 729.
(19) Gordon, M.; Taylor, J. S. *J. Appl. Chem.* **1952**, *2*, 1.
(20) Bonart, R.; Muller, E. H. *J. Macromol. Sci., Phys.* **1974**, *B10*, 177; **1974**; *B10*, 345.
(21) Koberstein, J. T.; Stein, R. S. *J. Polym. Sci., Polym. Phys. Ed.* **1983**, *21*, 2181.
(22) Koberstein, J. T.; Morra, B.; Stein, R. S. *J. Appl. Crystallogr.* **1980**, *13*, 34.
(23) Leung, L. M. Ph.D. Dissertation, Princeton University, Princeton, NJ, 1985.
(24) Xu, M.; MacKnight, W. J.; Chen, C. H. Y.; Thomas, E. L. *Polymer* **1983**, *24*, 1327.
(25) Simha, R.; Boyer, R. F. *J. Chem. Phys.* **1962**, *37*, 1003.
(26) Coleman, M. M.; Skrovanek, D. J.; Hu, J.; Painter, P. C. *Macromolecules* **1988**, *21*, 59.
(27) Sung, C. S. P.; Schneider, N. S. *Macromolecules* **1975**, *8*, 68.
(28) Dumais, J. J.; Jelinsky, L. W.; Leung, L. M.; Gancarz, I.; Galambos, A.; Koberstein, J. T. *Macromolecules* **1984**, *18*, 116.
(29) Eisenbach, C. D.; Hayen, H.; Nefzger, H. *Makromol. Chem., Rapid Commun.* **1989**, *10*, 463.

Registry No. (MDI)(BDO)(PPO) (block copolymer), 143495-45-8.